



An operando DRIFTS study of the active sites and the active intermediates of the NO-SCR reaction by methane over In,H- and In,Pd,H-zeolite catalysts

Ferenc Lónyi^{a,*}, Hanna E. Solt^a, József Valyon^a, Hernán Decolatti^b, Laura B. Gutierrez^b, Eduardo Miró^b

^a Institute of Nanochemistry and Catalysis, Chemical Research Center, Hungarian Academy of Sciences, Pusztaszeri u. 59-67, 1025 Budapest, Hungary

^b Instituto de Investigaciones en Catálisis y Petroquímica, INCAPE (FIQ, UNL-CONICET), Santiago del Estero 2829, 3000 Santa Fe, Argentina

ARTICLE INFO

Article history:

Received 31 May 2010

Received in revised form 16 July 2010

Accepted 22 July 2010

Available online 30 July 2010

Keywords:

In,H-zeolites

In,Pd,H-zeolites

NO-SCR by CH₄

Operando DRIFTS

ABSTRACT

Zeolites In,H-ZSM-5 (Si/Al = 29.7, 1.7 wt% In) and In,H-mordenite (In,H-M, Si/Al = 6.7, 3.5 wt% In) were prepared by reductive solid state ion exchange (RSSIE) method and studied in the selective catalytic reduction of NO (NO-SCR) by methane. The results suggested that the methane oxidation reactions proceed by redox type mechanisms over In⁺/InO⁺ sites. The NO reduction selectivity was shown to be related to the relative rates of In⁺ oxidation by NO and O₂. Regarding the relative rates, the In⁺ density of the zeolite was the most important. Above about 673 K the In,H-ZSM-5 (T-atom/In = 102) had higher NO reduction selectivity than the In,H-mordenite (T-atom/In = 46). The operando DRIFTS examinations suggested that NO⁺ and NO₃⁻ surface species were formed simultaneously on InO⁺Z⁻ sites, and were consumed together in the NO-SCR reaction with methane. The reduction of the NO₃⁻ by methane gave an activated N-containing intermediate, which further reacted with the NO⁺ species to give N₂. The NO-SCR properties could be significantly improved by adding small amount of Pd to the In,H-zeolite catalyst. The promoting effect of Pd was interpreted as a concerted action of InO⁺ and the Pd^{m+} sites. The interplay between these sites is twofold: the Pd speeds up the equilibration of the NO/O₂ mixture, thereby, increases the formation rate and the steady state concentration of the activated nitrate species, whereas the In⁺/InO⁺ sites prevent the transformation of Pd-nitrosyls to less reactive isocyanate and nitrile species.

© 2010 Elsevier B.V. All rights reserved.

1. Introduction

The selective catalytic reduction of NO_x with cheap and abundantly available methane in the presence of large oxygen excess (NO_x-SCR) is a feasible process to reduce the NO_x emission especially of boilers and engines, fuelled by natural gas [1–4]. The most efficient catalysts, which are able to activate the relatively stable methane molecule for the reaction, contain transition metals, such as, Pd, Co, Mn, Ni, Ga or In [2,4–7].

A number of studies suggest that indium-containing zeolites show significant activity in the NO_x-SCR [8–19]. The catalytic activity is generally attributed to cationic indium species [7–9,11,15–18] balancing the negative charge on the zeolite framework [7,20–23]. The activity and selectivity of the different In-zeolite catalysts show a large variety, suggesting that the activity depends also on the chemical environment of the active species [8,10,11,13–16,19].

The role of the zeolite structure and composition in generating NO-SCR activity is an important detail of the reaction mechanism.

According to our present knowledge the catalytic reaction cycle is introduced by the oxidation of NO to NO₂, the NO₂ reacts then with the catalyst forming an activated surface intermediate, such as NO₃⁻, that is able to oxidize methane [6,8,16–18,24]. It was shown that under the conditions of the NO-SCR reaction mainly InO⁺ cations balance the negative charges on the zeolite framework. The formation of the former activated surface intermediate is usually visualized as a simple NO₂ chemisorption over InO⁺ [8,16–18].

A second transition metal, such as Co [13,14], Ir [8], Pt [25] or Fe [19] in an indium-containing zeolite can significantly improve catalytic properties. It was suggested that the second metal can speed up the NO to NO₂ conversion (2NO + O₂ ⇌ 2NO₂) and, thereby, can accelerate the SCR reaction. It was shown, for instance, that the role of the iridium sites of Ir-promoted In,H-ZSM-5 catalyst was to accelerate the formation and chemisorption of NO₂ on the InO⁺ sites [8,26]. Such mechanism was not proved for any of the above mentioned promoting metals, although the synergism of the metals was clearly demonstrated. It is also unclear why a promoting metal improves the catalytic activity of some In/H-zeolite preparations, while has no effect on some other In,H-zeolite catalysts.

The present study point out that the NO-SCR reaction proceeds through NO⁺ and NO₃⁻ intermediates formed together over the indium oxocations of the In,H-zeolites. The NO⁺ is not able to oxidize methane, but participates in nitrogen forming reaction with

* Corresponding author at: Department of Micro- and Mesoporous Materials, Institute of Nanochemistry and Catalysis, Chemical Research Center, Hungarian Academy of Sciences, Pusztaszeri u. 59-67, 1025 Budapest, Hungary.
Tel.: +36 1 438 1162; fax: +36 1 438 1164.

E-mail address: lonyi@chemres.hu (F. Lónyi).

the N-containing activated intermediate obtained from the reaction of the NO_3^- and methane.

2. Experimental

2.1. Catalyst preparation

In,H-zeolite samples were prepared by the method of reductive solid state ion exchange (RSSIE). Zeolites H-mordenite (H-M, Süd-Chemie AG; $\text{Si}/\text{Al}_F = 6.7$, where Al_F means framework Al atom) and H-ZSM-5 (our synthetic product; $\text{Si}/\text{Al}_F = 33.0$) were mixed with In_2O_3 (Aldrich; 99.99%) applying intense co-grinding. The obtained $\text{In}_2\text{O}_3/\text{H-zeolite}$ mixtures were treated in H_2 flow at 773 K for 1 h, then cooled down to room temperature in He flow and finally oxidized in O_2 flow at 673 K. The Al_F/In ratio of the obtained mordenite and the ZSM-5 catalysts were 6 and 3, respectively. Catalysts, having 0.5 wt% Pd content, were prepared by impregnating the In,H-M and H-M samples with calculated amount of $\text{Pd}(\text{NH}_3)_4(\text{NO}_3)_2$ solution and by heating the impregnated samples in O_2 flow at 623 K for 4 h. The respective catalysts were designated as In,Pd,H-M and Pd,H-M.

2.2. Catalytic activity

Catalytic experiments were carried out using a flow-through microreactor. In a $30\text{ cm}^3\text{ min}^{-1}$ flow of He about 100 mg of catalyst was pre-treated at 773 K for 1 h, then cooled to 573 K. The catalytic activities were determined at temperatures between 573 and 873 K. The reaction was initiated by switching the He flow to a flow of 4000 ppm NO/4000 ppm $\text{CH}_4/2\%$ O_2/He mixture. The total flow rate of the reaction mixture was $100\text{ cm}^3\text{ min}^{-1}$ throughout the catalytic experiments corresponding to about a GHSV value of $30\,000\text{ h}^{-1}$. (The bed volume was calculated using catalyst bulk density of 0.5 g cm^{-3} .) The reactor effluent was analyzed with an on-line MS (VG ProLab, Fisher Scientific) provided with a quantitative analysis program. The concentrations of the component gases in the reactor effluent were continuously monitored. The instrument was calibrated using appropriate gas mixtures with known compositions. To avoid the difficulty coming from the overlapping $m/z = 28$ signal of N_2 and CO the conversion of NO to N_2 was calculated from the following equation:

Conversion of NO to N_2 (mol%)

$$= \frac{[\text{NO}]^0 - [\text{NO}] - [\text{NO}_2] - [\text{N}_2\text{O}]}{[\text{NO}]^0} \times 100\%$$

where $[\text{NO}]^0$ is the initial concentration of NO (4000 ppm), whereas $[\text{NO}]$, $[\text{NO}_2]$ and $[\text{N}_2\text{O}]$ are the concentrations of the corresponding components in the reactor effluent. Note that only a trace amount of NO_2 and N_2O could be detected throughout the catalytic experiments. The calculated conversion to N_2 and the N_2 yield, calculated from the intensity of the $m/z = 28$ MS signal showed smaller than 5% deviation. This is suggesting that CO formation, if any, was usually insignificantly low.

2.3. Temperature-programmed oxidation (TPO) experiments

About 70 mg of In,H-zeolite catalyst was prepared by the RSSIE method in situ in the flow-through microreactor. The microreactor was used for the temperature-programmed oxidation (TPO) experiments. The sample obtained at 773 K in H_2 was cooled to room temperature in He flow and then it was heated up in a $30\text{ cm}^3\text{ min}^{-1}$ flow of 10% O_2/He mixture at a rate of 10 K min^{-1} to 773 K. The reactor effluents were analyzed by an on-line MS. The consumption rate of O_2 was plotted as a function of temperature to get the O_2 -TPO

curve. In the NO-TPO experiment 3% NO/He mixture was used as an oxidizing gas. The formation rates of the products of NO reduction, such as N_2O and N_2 , were recorded as a function of temperature.

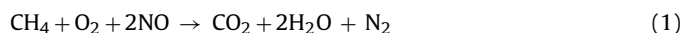
2.4. Operando DRIFTS investigations

The catalyst-bound surface species obtained from the NO_x -SCR reaction was studied by diffuse reflectance infrared Fourier transformation (DRIFT) spectroscopy using a Nicolet 5PC spectrometer, equipped with a COLLECTOR™ II diffuse reflectance mirror system and a high-temperature/high-pressure DRIFT spectroscopic reactor cell (Spectra-Tech, Inc.). Concentrations of the reactants and reaction products in the cell effluent were continuously monitored by an on-line MS. The sample cup of the cell was filled with about 20 mg of powdered sample. Prior to the NO_x -SCR experiments, catalyst samples were pre-treated in situ in a $30\text{ cm}^3\text{ min}^{-1}$ flow of 10% O_2/He at 773 K for 1 h, then purged with He and cooled to 573 K. The spectrum of the catalyst powder was taken at every selected reaction temperatures in He flow. This spectrum was subtracted from the corresponding spectrum of the catalyst and the reaction mixture in the cell. The resulting spectrum is referred to as difference spectrum. The activated catalyst was contacted with a flow of a gas mixture, containing either 4000 ppm NO/He, or 4000 ppm NO/2% O_2/He , or 4000 ppm NO/4000 ppm $\text{CH}_4/2\%$ O_2/He at temperatures in the range of 573–773 K. The GHSV was $\sim 30\,000\text{ h}^{-1}$. From here on these gas mixtures are referred to without giving the concentrations and indicating the presence of helium. The experimental set-up allowed abrupt switching between the reactant mixtures. The system reached a new steady state in about 4–8 min, as shown by the stabilized MS peak intensities. When studying the transient response of the system on the removal or admixing of an active gas component, the He concentration of the gas flow was adjusted accordingly to avoid partial pressure changes of the other gas components.

3. Results

3.1. Catalytic results

The H-ZSM-5 and H-M samples were inactive in the NO-SCR by CH_4 (not shown), whereas introduction of indium and/or palladium obviously generated active sites for the reaction (Fig. 1). The catalytic behavior of the In,H-ZSM-5 and In,H-M samples were, however, significantly different. Former sample showed high activity above 623 K up to the highest applied temperature (873 K), whereas the reaction hardly proceeded on the In,H-M in the same temperature range (Fig. 1A). Fig. 1B shows the conversion of methane in the same experiments. The conversion of methane was equal with the molar amount of formed CO_2 . If methane was selectively oxidized by NO the methane conversion had to be one fourth of the NO conversion ($\text{CH}_4 + 4\text{NO} \rightarrow \text{CO}_2 + 2\text{H}_2\text{O} + 2\text{N}_2$). However, the NO-SCR proceeded only in the presence of O_2 . With the participation of O_2 the reaction of NO reduction takes place according to the stoichiometry given by Eq. (1).



The curves of Fig. 1B show that the molar methane conversion was more than half of the NO conversion over most of the catalyst and at any temperature whereon the reaction proceeded, suggesting that a fraction of methane was converted to CO_2 in direct O_2 reduction ($\text{CH}_4 + 2\text{O}_2 \rightarrow \text{CO}_2 + 2\text{H}_2\text{O}$). From here on the reaction of Eq. (1) is referred to as NO reduction reaction, whereas the O_2 reduction is to be mentioned as methane combustion. Over the In,H-M catalyst, especially at higher reaction temperatures, the methane conversion significantly exceeded the stoichiometric methane demand of NO reduction (Eq. (1)). In contrast, over the

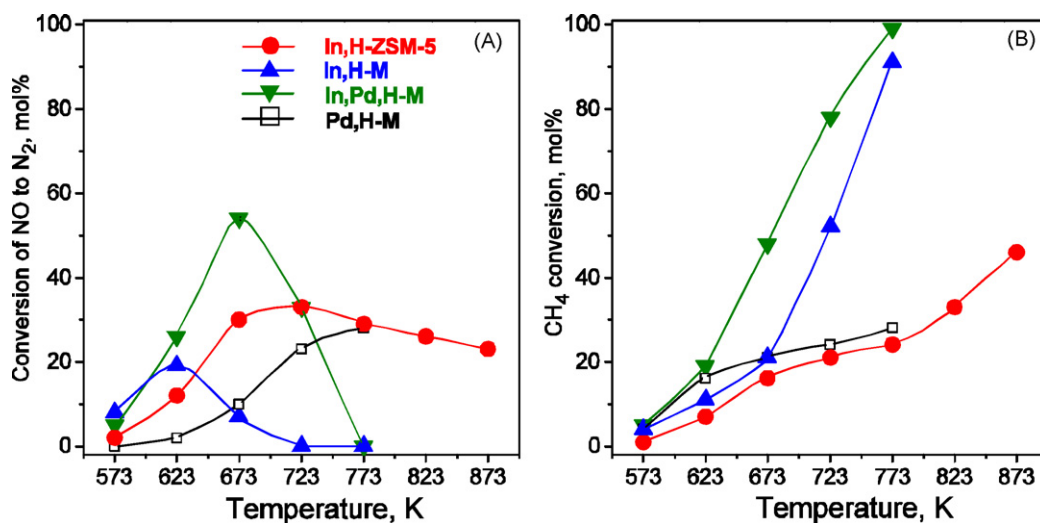


Fig. 1. The conversion of (A) NO to N₂ and (B) CH₄ over In,H-ZSM-5 (●), In,H-M (▲), In,Pd,H-M (▼), and Pd,H-M (□) in a 4000 ppm NO/4000 ppm CH₄/2% O₂/He gas mixture at GHSV 30 000 h⁻¹.

In,H-ZSM-5 sample the methane was consumed in the NO reduction reaction up to about 723 K. These results suggest that In,H-M activates O₂ for methane oxidation more effectively than the In,H-ZSM-5 catalyst.

Addition of small amount of Pd to In,H-M resulted in a surprisingly high NO-SCR activity in the temperature range of 623–723 K as compared to the corresponding zeolite, containing either In or Pd alone (Fig. 1A). The Pd additive increased the activity in methane oxidation not only by NO but also by O₂ (Fig. 1B). Over 723 K the SCR activity of the bimetallic In,Pd,H-M sample strongly decreased due to the extensive consumption of CH₄ by the undesired combustion reaction.

3.2. TPO measurements

Temperature-programmed oxidation (TPO) curves of the In,H-M and In,H-ZSM-5 catalysts were recorded using O₂ and NO as oxidizing agent (Fig. 2). The O₂-TPO curves clearly show that oxidation of the In,H-M takes place at temperature that is about 200 K lower than that of the In,H-ZSM-5 (Fig. 2A). Earlier reports confirmed that the RSSIE generates In⁺ cations that are oxidized by O₂ to species [In³⁺

O₂]⁺ [22,27]. A 2e reduction was attained in a subsequent H₂-TPR experiment, suggesting that the In⁺ state was recovered (not shown).

The concentration of NO in the NO-TPO effluent changes due to temperature dependent adsorption/desorption and conversion. The In⁺ oxidation was monitored by following the appearance of the NO oxidation products, such as N₂ and N₂O. It was found that the In⁺ was oxidized with NO both in In,H-ZSM-5 and In,H-M already below 373 K (Fig. 2B). The results suggest that the activation of NO or O₂ for catalytic methane oxidation proceeds with participation of In⁺/InO⁺ redox couple in the zeolite (vide infra). Because of the facile O₂ activation on the In,H-M zeolite, the O₂ effectively competes with the NO for the oxidation of methane under the SCR conditions. This provides explanation for the relatively low NO reduction selectivity of the In,H-M catalyst.

3.3. Surface species from adsorption of NO/O₂ mixture

DRIFT spectra obtained from adsorption of NO/O₂ mixture on H-ZSM-5 and H-M samples are shown in Figs. 3 and 4. The bands at 2128 and 1634 cm⁻¹ (Fig. 3B) stem from the ν_{NO} vibration of

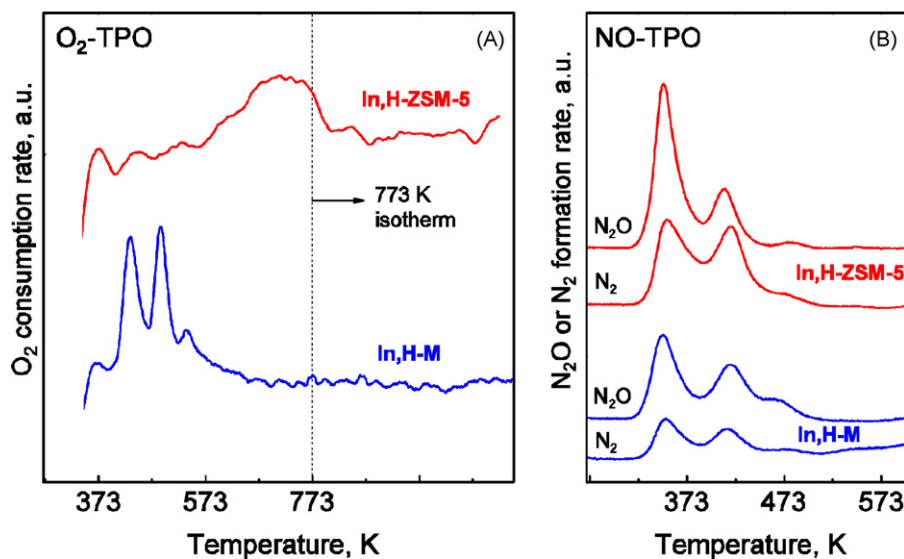


Fig. 2. Temperature-programmed oxidation (TPO) of In,H-ZSM-5 and In,H-M catalysts with (A) O₂ and (B) NO. The sample was prepared by the reductive solid state ion exchange method in situ in the TPO reactor by reducing In₂O₃/H-zeolite mixture in H₂ flow at 773 K.

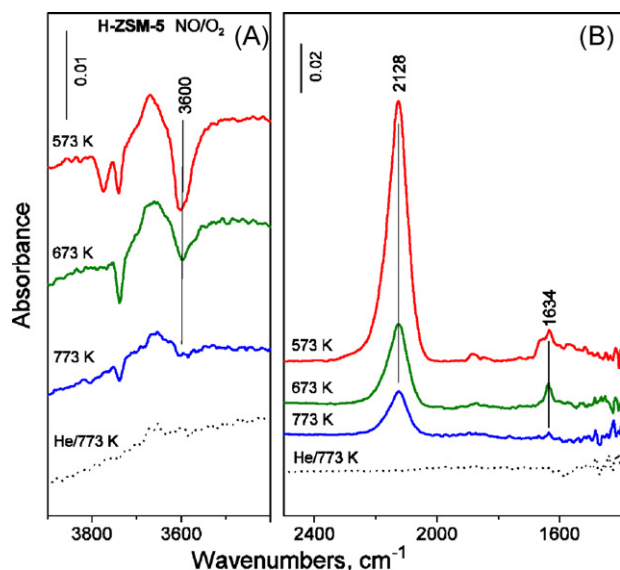
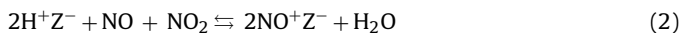


Fig. 3. DRIFT spectra of (A) the ν_{OH} region of H-ZSM-5 and (B) the surface species formed under continuous flow of 4000 ppm NO/2% O₂/He gas mixture at GHSV 30 000 h⁻¹ and the indicated temperature. The spectra were obtained from the same experiment at subsequently higher temperatures and after flushing the catalyst with pure He (dotted line).

nitrosonium ions (NO⁺) and the $\delta_{\text{H}_2\text{O}}$ vibration of water, respectively, bound to the H-ZSM-5 [28]. The formation of the adsorbed species was accompanied by the consumption of hydroxyl groups, as indicated by the corresponding negative OH bands in the difference spectrum (Fig. 3A). Previous studies [24,28–30] interpreted the corresponding spectral features by the process of Eq. (2):



where Z⁻ represents a segment of the zeolite framework carrying one negative charge. We note here that the intensity loss of the ν_{OH} band of the acidic hydroxyl groups is partly due to the replacement of the protons by NO⁺ and to some extent due to the H-bond interaction of the hydroxyl groups with water. The bands became weaker

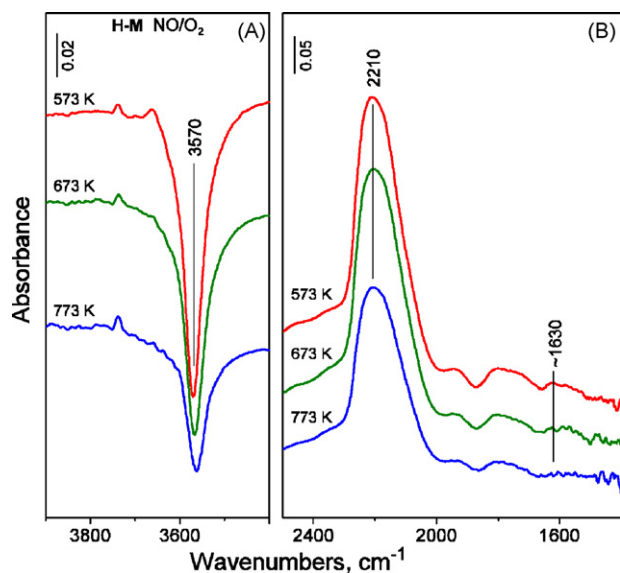


Fig. 4. DRIFT spectra of (A) the ν_{OH} region for H-M and (B) the surface species formed under continuous flow of 4000 ppm NO/2% O₂/He gas mixture at GHSV 30 000 h⁻¹ and the indicated temperature. The spectra were obtained from the same experiment at subsequently higher temperatures.

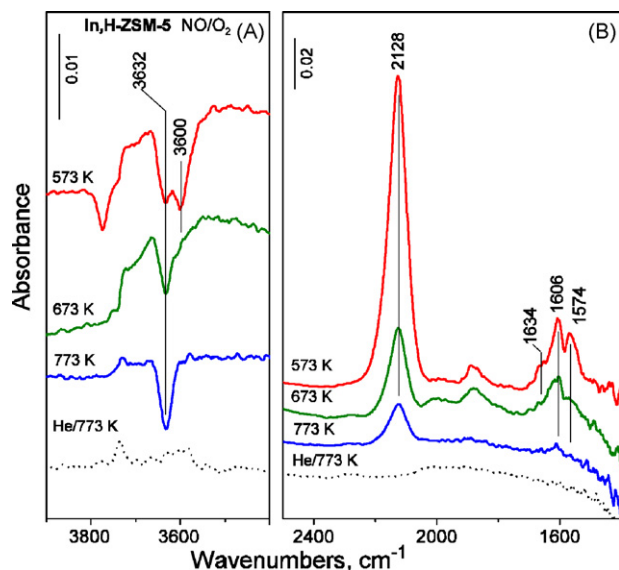


Fig. 5. DRIFT spectra of (A) the ν_{OH} region for In,H-ZSM-5 and (B) the surface species formed under continuous flow of 4000 ppm NO/2% O₂/He gas mixture at GHSV 30 000 h⁻¹ and the indicated temperature. The spectra were obtained from the same experiment at subsequently higher temperatures and after flushing the catalyst with pure He (dotted line).

if temperature was increased (Figs. 3 and 4) and became stronger if the temperature was lowered (not shown). All the adsorbed species were removed by a He flush at 773 K. These results show that the adsorption is relatively weak and reversible.

The NO/O₂ adsorption properties of the H-M sample were similar to that of the H-ZSM-5. The formation of NO⁺ and water was again simultaneous (Fig. 4). The adsorbed H₂O generated three broad bands, the so called ABC triad, around 2860, 2380, and 1700 cm⁻¹. Only the latter two are discernible in the frequency range, shown in Fig. 4B [31,32]. There is a weak $\delta_{\text{H}_2\text{O}}$ band at about 1630 cm⁻¹. The NO⁺ species gave broad band around 2210 cm⁻¹. The concentration of NO⁺ species decreased, if temperature was raised, however the decrease was much smaller than in the case of the H-ZSM-5 (cf. Figs. 3B and 4B) indicating a more effective stabilization of NO⁺ in the mordenite than in the ZSM-5. The H-mordenite has two different kinds of bridged hydroxyl group: one, located in main channels and another in the side pockets, giving ν_{OH} bands at 3610 and 3575 cm⁻¹ (vide infra). The negative OH band in the difference spectrum at about 3570 cm⁻¹ suggests that the adsorption of the NO/O₂ mixture induced dehydroxylation only in the side pockets.

The In,H-ZSM-5 and In,H-mordenite zeolites showed spectral features resembling to those of the H-forms; however, some additional bands also appeared. These bands are at 3632 cm⁻¹ (negative band) and at 1606 and 1574 cm⁻¹ (positive bands) (Fig. 5), and at ~3645 cm⁻¹ (shoulder on the negative band) and at 1612 and 1575 cm⁻¹ (positive bands) (Fig. 6). The positive bands in the 1630–1550 cm⁻¹ range are generally considered to come from the adsorption of NO₂ on InO⁺ sites [8,15,17,18,24]. Nitrate species usually give rise to a characteristic absorption band in the spectral ranges of 1650–1600 cm⁻¹ (bridging bidentate nitrate), 1585–1500 cm⁻¹ (chelating bidentate nitrate), and 1530–1480 cm⁻¹ (monodentate nitrate) [33,34]. Accordingly, we attribute the bands at 1612–1606 cm⁻¹ and at about 1575 cm⁻¹ to bridging and chelating bidentate nitrate and nitrate species, respectively (Figs. 5 and 6). The assignment of bidentate nitrate was supported by density functional calculations [35,36]. For supporting our assignment to nitrate we mention that similar bands, developed from the adsorption of NO/O₂ mixture on Cu,H-ZSM-5

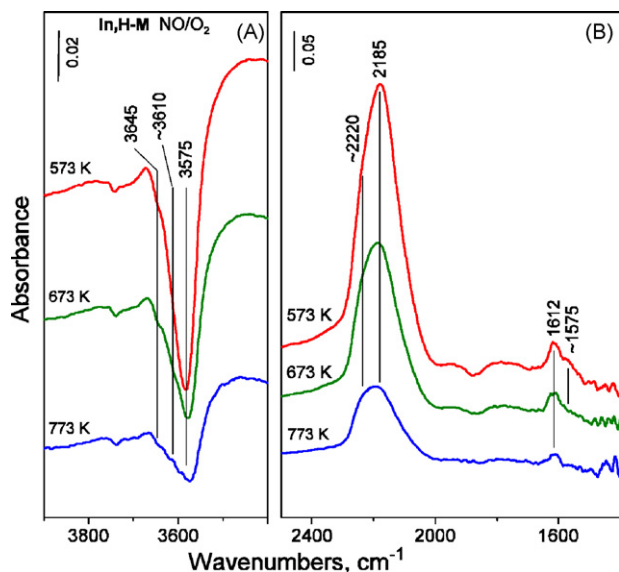


Fig. 6. DRIFT spectra of (A) the ν_{OH} region for In,H-M and (B) the surface species formed under continuous flow of 4000 ppm NO/2% O_2 /He at GHSV 30 000 h^{-1} and the indicated temperature. The spectra were obtained from the same experiment at subsequently higher temperatures.

[37], Co,H-ZSM-5 [38] and Fe,H-ZSM-5 [33] and were assigned also to NO_3^- . The firm assignment of these bands to a specific species is difficult because the wave number range below about 1300 cm^{-1} is strongly obscured by the absorption of the zeolite matrix.

The negative band at 3632 cm^{-1} (Fig. 5A) and at 3645 cm^{-1} (Fig. 6A) provides evidence for the involvement of InO^+ species in the formation of nitrate species. The ν_{OH} bands in the range of $3630\text{--}3690\text{ cm}^{-1}$ come from the absorption of polarized or heterolytically dissociated H_2O in the electrostatic field of cations, such as, Co^{2+} [30,39], Fe^{2+} [40,41] or Cu^{2+} [42]. The InO^+ oxocations are also able to coordinate water at temperature as high as 570 K [21,22]. In accordance with earlier studies [39,40] the intensity loss of the OH bands in the $3630\text{--}3690\text{ cm}^{-1}$ range, moreover, the appearance of NO^+ and nitrate bands is a clear indication that the coordinated H_2O molecules were replaced by NO^+ and nitrate. Thus, a mechanism is effective over the In,H-zeolites, which provides NO^+ with concomitant nitrate formation in a reaction which is different of Eq. (2). However, this mechanism generate somewhat different species in the In,H-ZSM-5 and In,H-mordenite. In the ZSM-5 the NO^+ gives a single band at 2128 cm^{-1} whereas in the mordenite it gives bands at 2185 and 2220 cm^{-1} (Figs. 5B and 6B). Nitrate bands are present in the spectrum of both samples at 1574 and at about 1610 cm^{-1} .

At 673 K and above there is hardly any negative ν_{OH} band of acidic OH-groups and $\delta_{\text{H}_2\text{O}}$ band in the difference spectrum of the In,H-ZSM-5 (Fig. 5). The lack of adsorption induced dehydroxylation and the absence of adsorbed water suggests that virtually no NO^+ species was formed according to Eq. (2) in this sample or, if formed, it was not retained at these temperatures.

The two kinds of NO^+ species in the In,H-M sample is related to two different kinds of adsorption interactions. From the results obtained for the H-M we concluded that exchange of the protons in the side pockets by NO^+ brings about a ν_{NO} band near to 2220 cm^{-1} and a negative ν_{OH} band at 3575 cm^{-1} (vide ultra, Fig. 4). The same surface events were observed using the In,H-M sample, suggesting that one of the NO^+ species was located in the side pockets (Fig. 6). The results also suggest that the other NO^+ band at 2185 cm^{-1} was generated with the involvement of InO^+ species. In a previous study it was shown that the NO^+ in the main channels and the side pock-

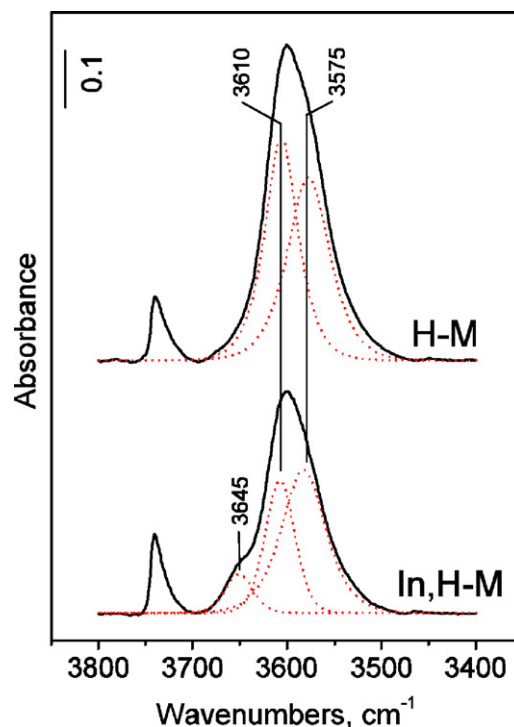


Fig. 7. DRIFT spectra of the ν_{OH} region for H-M and In,H-M (solid curves). The spectra were recorded in He flow at 573 K. Dotted lines indicate the component bands obtained by a curve fitting computer program.

ets has different vibration frequencies [32]. A fraction of the NO^+ species is most probable present in the main channel where the InO^+ ions are also localized. The results shown in Fig. 7 provide additional evidence for this localization. The 3610 cm^{-1} band is weaker in the In, H-M than in the H-M relative to the 3575 cm^{-1} band of the corresponding sample. It follows that InO^+ must occupy ion exchange positions mainly in the main channels of mordenite and substantiates that the NO^+ species, giving the 2185 cm^{-1} band, balance positive framework charges in the main channels. The relatively smaller contribution of the former reaction route to the NO^+ formation in the main channels is evidenced by the moderate water formation, indicated by the low intensities of the broad bands at ~ 2380 , and 1700 cm^{-1} (B and C bands from the ABC triad [31]) characteristic of adsorbed water and the absence of negative ν_{OH} band at about 3610 cm^{-1} (Fig. 6B). The involvement of InO^+ explains the appearance of the nitrate bands. The thermal stability of these two NO^+ species is not much different (Fig. 6B).

In addition to those mentioned above a new species was formed on the In,Pd,H-M, as indicated by the appearance of a new band at 1870 cm^{-1} (cf. Figs. 6B and 8B), if the sample was contacted with flow of NO/O_2 mixture. The band is characteristic for $\text{Pd}^{2+}\text{-NO}$ complexes [43–45]. Note that this band is superimposed on a broader band, which becomes stronger as the temperature is increased. The origin of this band is unknown at present. Nevertheless, the results clearly show that the $\text{Pd}^{2+}\text{-NO}$ species has high thermal stability. The intensities of the NO_3^- bands at 1615 and $\sim 1575\text{ cm}^{-1}$ somewhat increased relative to the intensity of the NO^+ bands. If O_2 input was stopped (the sample was flushed with NO/He flow) the $\text{Pd}^{2+}\text{-NO}$ concentration increased on expense of the concentration of the nitrosonium ions and the nitrates (Fig. 8B, cf. solid and dotted line spectra). Other researchers have already reported about similar findings [24,28,30]. The results suggest that the $\text{Pd}^{2+}\text{-NO}$ with O_2 could transform to NO_2 [29], and, finally, to nitrate.

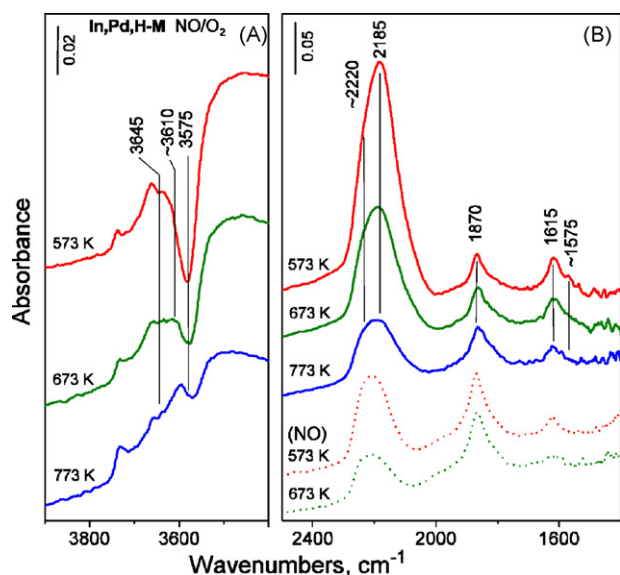


Fig. 8. DRIFT spectra of (A) the ν_{OH} region for In,Pd,H-M and (B) the surface species under continuous flow of 4000 ppm $\text{NO}/2\% \text{O}_2/\text{He}$ at GHSV 30 000 h^{-1} and the indicated temperature. Before the dotted line spectra were recorded the gas mixture was deprived from O_2 and the He concentration was adjusted to maintain the NO partial pressure. The spectra were obtained from the same experiment at subsequently higher temperatures.

3.4. The reaction of methane with the species obtained from NO/O_2

After the steady state of the zeolite/ NO/O_2 system was established at 573 K methane was admixed to the gas flow. The sharp band centered at 3014 cm^{-1} and the rotational side bands clearly indicate the appearance of methane in the gas phase above the catalysts. The methane concentration increased from zero up to a steady concentration in about 6–8 min. The composition of the DRIFTS reactor effluent and the DRIFT spectrum of the H-zeolite, In,H-zeolite, Pd,H-zeolite, and In,Pd,H-zeolite samples were monitored (Figs. 9–12). With methane in the gas mixture a lower steady state concentration of the active adsorbed species were established. The extent and rate of the change was found to reflect the activity of the catalyst.

The H-ZSM-5 and the H-M catalysts behaved somewhat differently. The methane left the H-M sample, wherein the NO^+ is well stabilized in the side pockets, unchanged (Fig. 9A). In contrast, the concentration of the NO^+ , bound in the H-ZSM-5 (band at 2128 cm^{-1}), slowly decreased (Fig. 9B). However, SCR products, such as CO_2 and N_2 , were not detected in the gas phase. In lack of reaction products the decrease of the NO^+ concentration can be attributed only to the reversal of the reaction according to Eq. (2). The non-reactivity of NO^+ surface species with methane is in accordance with the inactivity of the H-form zeolites in the NO_x -SCR with methane.

The methane slowly removed the NO^+ from both In,H-zeolite catalysts (Fig. 10). The NO^+ removal was much faster from the In,H-ZSM-5 than from the In,H-M. Obviously, the erosion of the NO^+ and the NO_3^- bands of the In,H-ZSM-5 catalyst, occurred together (Fig. 10B). It is rational to think that the concomitantly formed surface species (NO^+ and NO_3^-) are preferentially removed parallel. Most importantly, the consumption of these species occurs with the formation of CO_2 (bands at 2362 and 2332 cm^{-1} in the IR spectra, and also detected by MS) and N_2 (detected by MS). It should be noted that, after an initial increase, the concentrations of CO_2 and N_2 started to decrease in the reactor effluent together with the decreasing concentration of the reactive surface species until

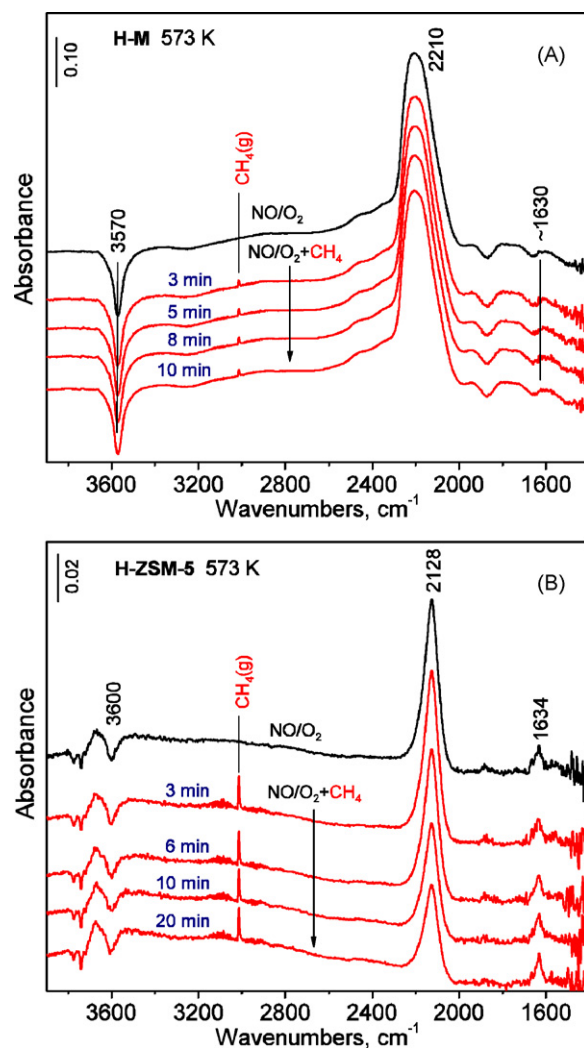


Fig. 9. Operando DRIFTS examination of the transient response of the H-zeolite/reactant systems on the change of reactant composition. The zeolites (A) H-M and (B) H-ZSM-5 were contacted with the gas flow of 4000 ppm $\text{NO}/2\% \text{O}_2/\text{He}$ at GHSV 30 000 h^{-1} and 573 K until the steady state was established (uppermost spectrum), then the flow was abruptly changed to a flow of 4000 ppm $\text{NO}/4000$ ppm $\text{CH}_4/2\% \text{O}_2/\text{He}$. Spectra were recorded after the indicated time on the stream.

a new steady state was established (Fig. 10B). A very similar picture emerges for In,H-M catalyst (Fig. 10A). The methane resulted in the intensity loss of the NO^+ band at $\sim 2180 \text{ cm}^{-1}$ and the nitrate bands at 1615 and 1580 cm^{-1} . Notice, that these are the bands of species, which were formed together in the main channels without the participation of bridged hydroxyl groups. The elimination of these adsorbed species by methane was accompanied again by the formation of the SCR products, such as CO_2 (Fig. 10A, spectra 3 to 10 min) and N_2 . The NO^+ , formed with the participation of bridged hydroxyl groups (Eq. (2)), was stabilized in the side pockets (band at $\sim 2210 \text{ cm}^{-1}$) and did not react with methane.

The initial concentration of the adsorbed NO_3^- was found to be somewhat higher in the In,Pd,H-M catalyst than in the corresponding In,H-M catalyst (cf. Figs. 10A and 11). The methane in the gas mixture slowly brings away a fraction of all the species from the In,Pd,H-M catalyst, including the Pd^{2+} -bound nitrosyl group (ν_{NO} band at 1870 cm^{-1}) (Fig. 11). The steady state NO_x coverage of the catalyst was lower at 673 K than it was at 573 K. Moreover, a larger fraction of these species was removed until the new steady state was established with the methane in the gas mixture (Fig. 12A). In agreement with the results shown in Fig. 1A the NO conversion

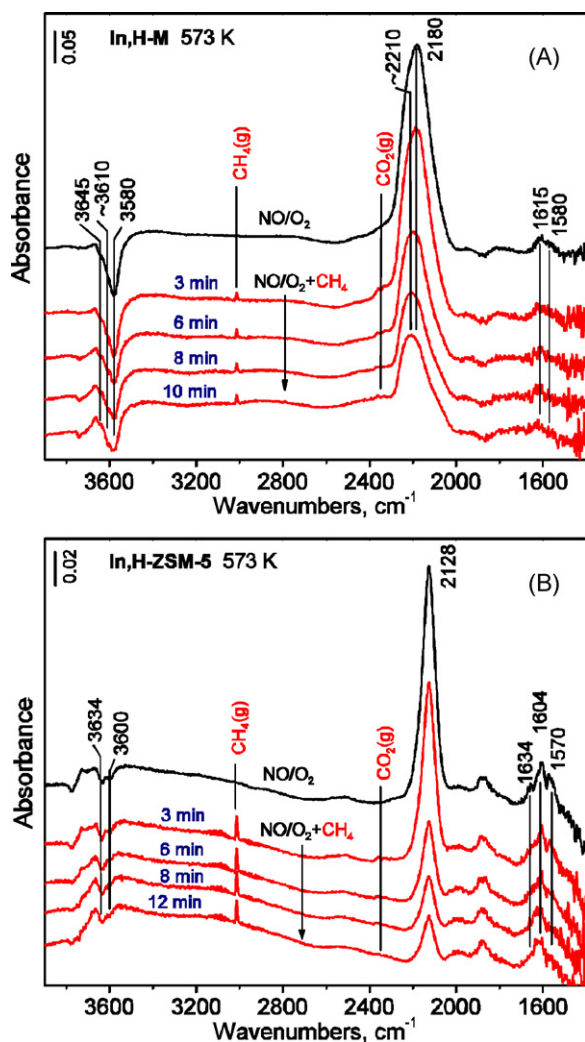


Fig. 10. Operando DRIFTS examination of the transient response of the In,H-zeolite/reactant systems on the change of reactant composition. The zeolites (A) In,H-M and (B) In,H-ZSM-5 were contacted with the gas flow of 4000 ppm NO/2% O₂/He at GHSV 30 000 h⁻¹ and 573 K until the steady state was established (uppermost spectrum), then the flow was abruptly changed to a flow of 4000 ppm NO/4000 ppm CH₄/2% O₂/He. Spectra were recorded after the indicated time on the stream.

was higher at the higher temperature. It is worth to note that the methane affected also the NO⁺ species in the side pockets (component band at ~2220 cm⁻¹). Would this mean that these species can also react with methane, but only at higher temperature? It seems more likely that the higher methane conversion generates enough water to decrease the NO⁺ coverage by pushing back the reaction of Eq. (2). When methane was removed from the reactant mixture the first spectrum was fully restored. Upon depriving the gas flow also of NO all the nitrosyl started to lose intensity. Interestingly, the bands of NO₃⁻ at 1617 and 1570 cm⁻¹ first gained intensity then started to weaken (Fig. 12A, hatched areas). The change of the nitrate coverage is probably related to conversion of the Pd nitrosyl with O₂ to NO₂ and finally to NO₃⁻. In absence of NO in the gas the equilibrium of Eq. (2) is pushed to the left. This process feeds the NO₂ generation reaction on the palladium with NO. The nitrosyl coverage of the palladium began to drop with a delay when the NO resource of the catalyst became exhausted.

The NO⁺ species were shown to be located predominantly in the side pockets of the H-mordenite and the concentration of the bound NO₃⁻ is negligible (vide ultra). In this respect the Pd,H-M sample behaves very similarly to the H-M sample (Fig. 12B). A dif-

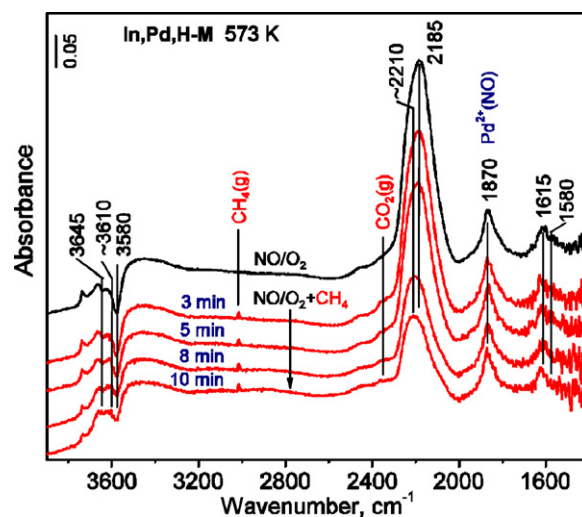


Fig. 11. Operando DRIFTS examination of the transient response of the In,Pd,H-M/reactant system on the change of reactant composition. The zeolites In,Pd,H-M was contacted with the gas flow of 4000 ppm NO/2% O₂/He at GHSV 30 000 h⁻¹ and 573 K until the steady state was established (uppermost spectrum), then the flow was abruptly changed to a flow of 4000 ppm NO/4000 ppm CH₄/2% O₂/He. Spectra were recorded after the indicated time on the stream.

ference is the appearance of the ν_{NO} band of the Pd²⁺(NO) species (band at 1865 cm⁻¹). Introduction of methane into the NO/O₂ flow gradually removed the Pd²⁺(NO) species, while isocyanate (NCO⁻) and nitrile (CN⁻) species were formed, as indicated by the evolution of bands at 2283, 2206, and 2154 cm⁻¹. The isocyanate, giving the higher frequency band(s), seems to be the dominating species [24,34,46]. When methane was removed from the reactant mixture the band of NO⁺ (2220 cm⁻¹) was restored, but not the band of the Pd²⁺(NO) (Fig. 12B). This behavior is much different from that of the In,Pd,H-M catalyst (cf. Fig. 12A and 12B). The restored NO⁺ was also eliminated when the gas flow was deprived also of NO (only O₂/He flow left), whereas the isocyanate and nitrile species (bands at 2283, 2206, and 2154 cm⁻¹) were retained under the applied conditions (Fig. 12B).

4. Discussion

4.1. Zeolite structure and activity

The relative weight of the NO reduction (Eq. (1)) and the direct methane combustion reactions, i.e., the selectivity, depends on both the temperature and the catalyst. Fig. 1 shows that, over all the examined catalysts, the methane conversion increased when the reaction temperature was increased, whereas the NO conversion passed through a maximum. The increase of CH₄ conversion was especially fast in the temperature range where the NO conversion started to drop. This infers that combustion became the main route of methane conversion in this temperature range.

The origin of the different TPO peaks is not clear yet but it is obvious that the oxidation of the In⁺ in the mordenite catalyst was accomplished at lower temperature than in the ZSM-5 catalyst (Fig. 2). The lower CH₄ combustion activity and the higher NO reduction selectivity at higher temperatures (and conversions) seem to come from the hindered oxidation of the In⁺ cations by O₂ in the ZSM-5 catalyst. Previous studies substantiated that O₂ converts In⁺ to InO⁺ cations [22,27]. Since the reaction requires the transfer of 4e from two In⁺ ions to two O atoms (Eq. (3)), it is rational to think that the oxidation of the In,H-M catalyst, having a higher indium concentration (T-atom/In=46) and, as a consequence, shorter In⁺ to In⁺ distances, is more facile than

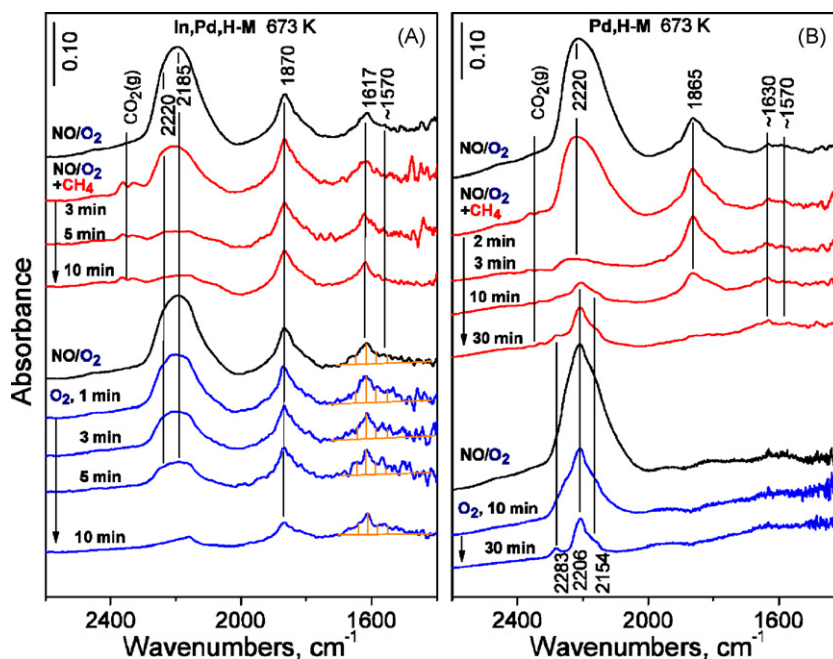


Fig. 12. Operando DRIFTS examination of the transient response of the In,Pd,H-zeolite/reactant systems on the change of reactant composition. The zeolites (A) In,Pd,H-M and (B) Pd,H-M were contacted with the gas flow of 4000 ppm NO/2% O₂/He at GHSV 30 000 h⁻¹ and 673 K until the steady state was established (uppermost spectrum), then the flow was abruptly changed to a flow of 4000 ppm NO/4000 ppm CH₄/2% O₂/He. Spectra were recorded after the indicated time on the stream. Then, the gas flow was changed again for the NO/O₂ mixture. After a new steady state established a spectrum was recorded and the gas flow was replaced by a flow of 2% O₂/He mixture. Spectra were recorded again after the indicated time on the O₂/He stream.

oxidation of the In,H-ZSM-5 catalyst, having a lower In content (T-atom/In = 102) and, most probably, higher distances between the In⁺ ions.



The results presented in Figs. 6 and 7 substantiated that some of the In⁺ ions are located in the 8-membered ring (8MR) side pockets of mordenite. In contrast to our expectation, the In⁺ ions were easier to oxidize in the hard-to-access side pockets of mordenite than in the more accessible 10MR channels of the ZSM-5 (Fig. 2A). This finding supports the notion that the kinetics of O₂-oxidation depends more on the In⁺ concentration than on the environment of the cation.

In contrast to the O₂-TPO, the NO-TPO was equally facile at lower and at higher In⁺ concentrations. The NO-TPO profile hardly depended on the zeolite structure. Both N₂O and N₂ were observed as product (Fig. 2B) suggesting that the oxidation of In⁺ can occur in two reactions (Eqs. (4a) and (4b)) with the transfer of 2e to an oxygen atom in either of the reactions.

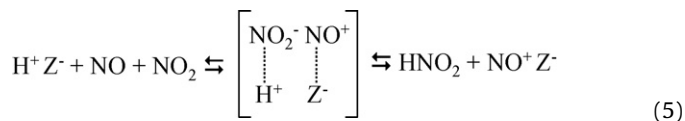


In most previous studies the In-zeolite catalyst preparations contained In and Al_F in about molar equivalence. High silica In-zeolites were found to be relatively low activity but high selectivity [10,15–17]. In contrast, the In-zeolite having low Si/Al ratio were of poor selectivity [14,47]. The results discussed above suggest that the high In density, in conjunction with low Si to Al ratio, is responsible for the unfavorable catalytic properties.

4.2. Surface species from NO/O₂ mixture

The O₂, which is present in the NO/CH₄/O₂ mixture in high concentration relative to the NO and CH₄, oxidizes NO to NO₂. The equilibrium NO and NO₂ concentration of the reacting gas is determined by the temperature. The charge separation of NO and NO₂

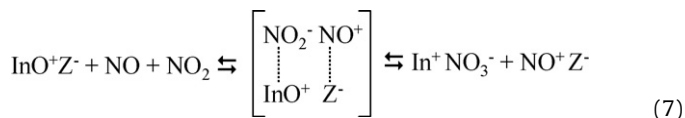
in the electrostatic field of the zeolite pores is well documented [28,48,49]. In the H-zeolites the nitrosonium and nitrite ion pair is transition state, which relaxes through reaction with zeolite hydroxyl groups. As a result the zeolite becomes dehydroxylated and nitrosonium ions balance the negative framework charge [28] (Eqs. (5) and (6)).



Our results suggest that the participation of the side pocket hydroxyls of the mordenite is preferred in the above reaction. The negative OH band at 3570 cm⁻¹ (Fig. 4A) suggests that the generation of NO⁺ cations under the applied experimental conditions eliminates mainly side pocket hydroxyls. This infers that the band at 2210 cm⁻¹ (Fig. 4B) stems from NO⁺ in the side pockets. This assignment is in harmony with that of Henriques et al. [32].

Unlike H-zeolites the transition metal zeolite catalysts initiate the formation of surface nitrate in contact with NO/O₂ mixture [37,50,51]. The details of the nitrate formation process on the In-zeolites are, however, not so clear yet [8,18,24,26]. None of the previously outlined mechanisms explain how the electric neutrality of the system is maintained along the process of NO₃⁻ generation. Some works simply describe the gas-solid interaction as adsorption resulting in an InO⁺-NO₂ [8,16–18]. However, there are spectroscopic evidences for nitrate formation. Recently it was suggested that first NO⁺ species are generated on the acidic hydroxyl groups according to Eq. (2). The NO⁺ reacts then with the oxocation to get surface nitrate [24]. Density functional calculations substantiated that NO₃⁻ complex can readily form in the reaction of NO₂ and zeolite oxocations, such as InO⁺ [35,36]. This infers that the oxidation of NO to NO₂ is a crucial first step of the nitrate formation process.

Note that ions with enough positive charge must be available to balance the negative charge of the zeolite framework and that of the nitrate anions. The In,H-zeolites of the present study contain both InO^+ and H^+ cations. It is possible therefore, that NO^+ is formed on the hydroxyl groups according to the mechanism given by Eqs. (5) and (6). The results of this study suggested that there is also another route whereon the NO^+ is formed together with the NO_3^- in reaction of an NO/NO_2 and the InO^+ species (Eq. (7)).



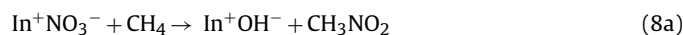
The simultaneous NO^+ and NO_3^- formation is a clear indication that InO^+ was involved in the process of NO^+ formation (Eq. (7)). When only NO^+ and no NO_3^- was generated the process had to proceed with the participation of hydroxyl groups (Eqs. (5) and (6)).

The NO^+ in the In,H-ZSM-5 gives a single stretching vibration band. Regardless of the formation mechanism the chemical environment of all the NO^+ species must be similar within the In,H-ZSM-5 structure, as suggested by the found single NO^+ stretching vibration band. The two bands of mordenite-bound NO^+ have to correspond to two different species. The oxocations were shown to be located in the main channels of mordenite, whereas the cationic sites of the side pockets are populated mainly by protons (Fig. 7). It is most probable that the NO^+ , giving a band at 2185 cm^{-1} , was formed according to Eq. (7) and was coordinated to the zeolite framework in the main channels.

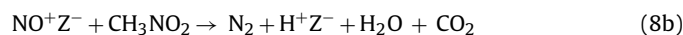
Concomitant formation of NO^+ and NO_3^- has been observed before also in zeolites having Co^{2+} [30], Na^+ [32], or Ba^{2+} [52] sites. The reaction was suggested to proceed via N_2O_4 disproportionation ($2\text{NO}_2 \rightleftharpoons \text{N}_2\text{O}_4 \rightleftharpoons \text{NO}^+ + \text{NO}_3^-$). This mechanism, which is different from that of Eq. (7), was substantiated because these metal cations do not carry extra-framework oxygen (EFO), they are virtually non-reducible and, therefore, cannot oxidize the NO_2^- to NO_3^- . In contrast, the oxocations of the In-zeolites are reducible. According to Eq. (7) the 2e reduction of the In^{3+} is paralleled by the oxidation of two nitrogen atoms in the NO and NO_2 , each by 1e.

From the adsorption of NO/O_2 mixture NO^+ was obtained over H-zeolites. However the H-zeolites were inactive in the NO-SCR reaction by methane. This infers that NO^+ is either not the active intermediate of the NO-SCR reaction [29] or it can be only one of the active intermediates needed to initiate the reaction with methane. The nitrogen of NO^+ has a formal oxidation state of +3. It has to react with compounds containing nitrogen atoms in the -3 formal oxidation state to get N_2 . Because the formation of NO^+ is quite facile the generation of an active intermediate, having nitrogen in the -3 oxidation state, seems to be prerequisite of the NO conversion to N_2 [30,52,53]. Methane has to be activated that latter active intermediate could be formed. This is probably the most hindered elementary step of the NO-SCR reaction [53–55]. Previous studies suggested that the zeolite-bound nitrate can oxidize methane and generate the desired intermediate. The reaction between methane and NO_3^- can provide organic nitro, nitrito, nitroso compounds, such as nitrosomethane (CH_3NO) and nitromethane (CH_3NO_2), isocyanate (NCO^-), nitrile (CN^-), or NH_x species (NH_3 or NH_4^+) [51, and references cited therein]. Under reaction conditions the consumption rate constant of the active intermediate is large relative to the rate constant of its formation. Therefore, it is difficult to detect the active intermediate and to get experimental evidence for its participation in the reaction. In lack of direct evidence any of these compounds can be the active intermediate of the NO-SCR reaction. Nitromethane has been substantiated to be the most probable one [50,53,54]. We monitored the reaction of the surface nitrate with gas phase methane (Figs. 10 and 11), but we could not observe

catalyst-bound isocyanate-, nitrile-, or NH_x species. However, it became obvious that the NO^+ and the NO_3^- co-generated over the In,H-zeolites play important role in the N_2 formation. The species formed together were consumed also together when the catalyst was exposed to methane (Figs. 10 and 11). The found involvement of NO^+ in the N_2 formation step is in contrast with that often suggested mechanism which concerns the reaction of gas phase or adsorbed NO or NO_2 with one of the above mentioned active intermediates to give N_2 [37,50,51]. These suggested mechanistic pictures do not involve the important details, how the oxidation state of the N atoms are changing to get finally N_2 [52,53]. The oxidation state of the N atoms in the NO^+ and the NO_3^- , formed together on an InO^+Z^- pair site (Eq. (7)) are +3 and +5, respectively. Thus, the NO^+ is ready to react with another intermediate formed nearby in the reaction between the indium nitrate and the methane. In the reaction of nitrate and methane, the active site must be regenerated to close the catalytic cycle. Accepting the suggestion that nitromethane, CH_3NO_2 , is one intermediate of the NO_x -SCR reaction with methane [50,53,54], the catalytic cycle is envisioned as follows (Eqs. (8a)–(8d)):



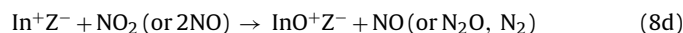
One can speculate that the N_2 formation step is the reaction between the NO^+ , formed according to Eq. (7), and the nitromethane (Eq. (8b)).



Note that the reaction of Eq. (8c) was proved to proceed, being the reaction route of the RSSIE. The RSSIE method was applied here to produce the In,H-zeolite samples [27].



The TPO results show that the oxidation of In^+ cations to InO^+ active sites by NO proceeds well below the lowest SCR temperature (573 K). The oxidation reaction regenerates the InO^+ active sites and completes the catalytic cycle.



Earlier we suggested a similar site regeneration mechanism for the Co,H-zeolite catalyst of the reaction [30]. The elementary steps of the methane oxidation reaction (Eq. (8a)) are presently not known. It has been proposed that the activation of methane (C–H bond cleavage) is initiated by adsorbed NO_2 , resulting in a methyl radical, adsorbed NO and a hydroxyl radical (or HONO , HNO_2), although gas phase methyl radicals could not be detected [50,53,54,56]. Our data do not question the radical mechanism; however, the above proposed reactions seem to give plausible explanation how the charge balance of the system can be maintained during the methane activation in a redox type catalytic cycle.

4.3. The catalytic effect of Pd

It is generally found that transition metals, such as Pt [25], Ir [8,26], or Co [13], as well as some finely dispersed transition metal oxides, such as FeO_x [19] or CeO_x [47] promote the activity of the NO-SCR zeolite catalysts. These additives were suggested to increase the NO_2 concentration in the reactant mixture by speeding up the NO/O_2 equilibration. Thereby the NO-SCR reaction is also accelerated, because the NO_2 has better potential than the NO to get ahead oxygen in the competition for the reducing agent methane. Because of the higher NO_2 concentration, the rate of the rate determining C–H bond activation and the SCR reaction increases. The Pd was found to have a similar promoting effect. According to Eq. (7), the equilibrium is shifted to the right side if the formation rate of NO_2 increases, i.e., the result is a higher concentration of the active

indium nitrate. Ogura et al. [8,26] studied the analogues In,Ir,H-ZSM-5 catalyst and reported about similar findings. The nitrate formation was negligible on the Pd,H-zeolite, whereas it was promoted by the presence of Pd on the In,H-zeolites. The nitrate species are better stabilized by the In than by the Pd cations of the zeolite.

It should be mentioned that the promoting effect of Pd can be observed at reaction temperatures below about 723 K. At higher temperatures the CH₄ is mainly consumed in undesired combustion reaction. The In-rich In,H-M sample facilitates O₂ activation and combustion as discussed above in section 4.1.

The cooperation between Pd²⁺ and InO⁺ active sites, however, seems to be twofold. On one hand the Pd increases the nitrate concentration (see above), while, on the other hand the InO⁺ species prevent the transformation of Pd nitrosyl species into more stable and less reactive nitrile and isocyanate species (Fig. 12). The details of this latter process are presently not known, however it might be related to an oxygen transfer from the InO⁺ to Pd²⁺(NO), facilitating the oxidation of the nitrosyl to NO₂. In this sense, the bimetallic In–Pd/H-zeolite resembles the Wacker type oxidation catalysts.

5. Conclusions

Nitrosonium ions (NO⁺) can be formed in two different processes over In,H-zeolites. One of them proceeds with the participation of zeolite protons (H⁺Z⁻), whereas the other one with the participation of the InO⁺ active sites (InO⁺Z⁻). Latter process leads to simultaneous formation of NO⁺ and NO₃⁻ species. Only the nitrate species can oxidize methane to generate active intermediate for the NO-SCR reaction. This active intermediate reacts then, most probably, with the NO⁺, which is not reactive with methane at all, to generate N₂.

The activity of In,H-M in the SCR reaction decreases drastically over 673 K due to the acceleration of the undesired methane oxidation with O₂ (methane combustion). The catalytic combustion is faster than the catalytic methane oxidation by NO if the oxidation of the active site In⁺ to InO⁺ proceeds by O₂ preferentially to the oxidation by NO. Above 673 K the In,H-ZSM-5 catalyst shows better NO selectivity than the In,H-mordenite. The favorable low methane combustion activity is related to the In density that is lower in the In,H-ZSM-5 than in the In,H-M catalyst.

The NO-SCR properties of the In,H-zeolite catalysts could be significantly improved by introduction of a small amount of Pd into the catalyst. The positive effect is related to the concerted action of InO⁺ and Pdⁿ⁺ sites. On one hand the presence of Pd results in a higher concentration of In-nitrate, which is highly reactive with methane. On the other hand, the In⁺/InO⁺ redox sites prevent the transformation of nitrosyl species on the Pd sites to less reactive isocyanate and nitrile species.

Acknowledgements

The authors wish to thank to for the financial support of the Hungarian Research Fund (OTKA no. K-69052) and the National Office for Research and Technology (NKTH, GVOP project no. 3.2.1. 2004-04-0277/3.0). Thanks are also due to the Hungarian-Argentinean TÉT program (AR-4/08) that made this joint project possible.

References

- [1] V.I. Parvulescu, P. Grange, B. Delmon, *Catal. Today* 46 (1998) 233–316.
- [2] Y. Li, J.N. Armor, *Appl. Catal. B* 1 (1992) L31–L40.
- [3] Y. Li, P. Battavio, J.N. Armor, *J. Catal.* 142 (1993) 561–571.
- [4] E. Kikuchi, K. Yogo, *Catal. Today* 22 (1994) 73–86.
- [5] Y. Li, J.N. Armor, *J. Catal.* 145 (1994) 1–9.
- [6] B.J. Adelman, W.M.H. Sachtler, *Appl. Catal. B* 14 (1997) 1–11.
- [7] E. Kikuchi, M. Ogura, I. Terasaki, Y. Goto, *J. Catal.* 161 (1996) 465–470.
- [8] M. Ogura, M. Hayashi, E. Kikuchi, *Catal. Today* 42 (1998) 159–166.
- [9] M. Ogura, T. Ohsaki, E. Kikuchi, *Micropor. Mesopor. Mater.* 21 (1998) 533–540.
- [10] F.G. Requejo, J.M. Ramallo-López, E.J. Ledo, E.E. Miró, L.B. Pierella, *Catal. Today* 54 (1999) 553–558.
- [11] J.M. Ramallo-López, L.B. Gutierrez, A.G. Babiloni, F.G. Requejo, E.E. Miró, *Catal. Lett.* 82 (2002) 131–139.
- [12] T. Sowade, C. Schmidt, F.-W. Schütze, H. Berndt, W. Grünert, *J. Catal.* 214 (2003) 100–112.
- [13] A. Kubacka, J. Janas, E. Wloch, B. Sulikowski, *Catal. Today* 101 (2005) 139–145.
- [14] A. Kubacka, J. Janas, B. Sulikowski, *Appl. Catal. B* 69 (2006) 43–48.
- [15] T. Maunula, J. Ahola, H. Hamada, *Appl. Catal. B* 64 (2006) 13–24.
- [16] O.A. Anunziata, A.R. Beltramone, E.J. Ledo, F.G. Requejo, *J. Mol. Catal. A* 267 (2007) 272–279.
- [17] M. Ogura, M. Hayashi, E. Kikuchi, *Catal. Today* 45 (1998) 139–145.
- [18] A.N. Beltramone, L.B. Pierella, F.G. Requejo, O.A. Anunziata, *Catal. Lett.* 91 (2003) 19–24.
- [19] R. Serra, M.J. Vecchiotti, E. Miro, A. Boix, *Catal. Today* 133 (2008) 480–486.
- [20] V. Kanazirev, Y. Neinska, T. Tsoncheva, L. Kosova, in: R. von Ballmoos, J.B. Higgins, M.M.J. Treacy (Eds.), *Proc. 9th Int. Zeolite Conf.*, 1992, Montreal, Butterworth-Heinemann, London, 1993, pp. 461–468.
- [21] H.K. Beyer, R.M. Mihalyi, Ch. Minchev, Y. Neinska, V. Kanazirev, *Micropor. Mater.* 7 (1996) 333–341.
- [22] R.M. Mihalyi, H.K. Beyer, V. Mavrodinova, Ch. Minchev, Y. Neinska, *Micropor. Mesopor. Mater.* 24 (1998) 143–151.
- [23] V. Mavrodinova, M. Popova, M.R. Mihalyi, G. Pal-Borbely, Ch. Minchev, *Appl. Catal. A* 262 (2004) 75–83.
- [24] L. Li, N. Guan, *Micropor. Mesopor. Mater.* 117 (2009) 450–457.
- [25] J.M. Ramallo-Lopez, F.G. Requejo, L.B. Gutierrez, E.E. Miro, *Appl. Catal. B* 29 (2001) 35–46.
- [26] M. Ogura, E. Kikuchi, *Chem. Lett.* (1996) 1017–1018.
- [27] H. Solt, F. Lonyi, R.M. Mihalyi, J. Valyon, *J. Phys. Chem. C* 112 (2008) 19423–19430.
- [28] K. Hadjiivanov, J. Saussey, J.L. Freys, J.C. Lavalley, *Catal. Lett.* 52 (1998) 103–108.
- [29] L.J. Lobree, A.W. Aylor, J.A. Reimer, A.T. Bell, *J. Catal.* 181 (1999) 189–204.
- [30] F. Lonyi, J. Valyon, L. Gutierrez, M.A. Ulla, E.A. Lombardo, *Appl. Catal. B* 73 (2007) 1–10.
- [31] A. Zecchina, F. Geobaldo, G. Spoto, S. Bordiga, G. Ricchiardi, R. Buzzoni, G. Petrini, *J. Phys. Chem.* 100 (1996) 16584–16599.
- [32] C. Henriques, O. Marie, F. Thibault-Starzyk, J.-C. Lavalley, *Micropor. Mesopor. Mater.* 50 (2001) 167–171.
- [33] K. Hadjiivanov, *Catal. Lett.* 68 (2000) 157–161.
- [34] K.I. Hadjiivanov, *Catal. Rev.: Sci. Eng.* 42 (1–2) (2000) 71–144.
- [35] T. Kanougi, K. Furukawa, M. Yamada, Y. Oumi, M. Kubo, A. Stirling, A. Fahmi, A. Miyamoto, *Appl. Surf. Sci.* 119 (1997) 103–106.
- [36] T. Kanougi, H. Tsuruya, Y. Oumi, A. Chatterjee, A. Fahmi, M. Kubo, A. Miyamoto, *Appl. Surf. Sci.* 130–132 (1998) 561–565.
- [37] F. Poignant, J.L. Freys, M. Daturi, J. Saussey, *Catal. Today* 70 (2001) 197–211.
- [38] E. Ivanova, K. Hadjiivanov, D. Klissurski, M. Bevilacqua, T. Armaroli, G. Busca, *Micropor. Mesopor. Mater.* 46 (2001) 299–309.
- [39] L. Gutierrez, M.A. Ulla, E.A. Lombardo, A. Kovacs, F. Lonyi, J. Valyon, *Appl. Catal. A* 292 (2005) 154–161.
- [40] H.-Y. Chen, T. Voskoboinikov, W.M.H. Sachtler, *J. Catal.* 186 (1999) 91–99.
- [41] R. Brosius, P. Bazin, F. Thibault-Starzyk, J.A. Martens, *J. Catal.* 234 (2005) 191–198.
- [42] J. Valyon, W.K. Hall, *J. Phys. Chem.* 97 (1993) 7054–7060.
- [43] C. Desorme, P. Gelin, C. Lecuyer, M. Primet, *J. Catal.* 177 (1998) 352–362.
- [44] K. Shimizu, F. Okada, Y. Nakamura, A. Satsuma, T. Hattori, *J. Catal.* 195 (2000) 151–160.
- [45] K. Chakarova, E. Ivanova, K. Hadjiivanov, D. Klissurski, H. Knözinger, *Phys. Chem. Chem. Phys.* 6 (2004) 3702–3704.
- [46] M.H. Kim, I.-S. Nam, Y.G. Kim, *Chem. Commun.* 16 (1998) 1771–1772.
- [47] H. Berndt, F.-H. Schütze, M. Richter, T. Sowade, W. Grünert, *Appl. Catal. B* 40 (2003) 51–67.
- [48] P.H. Kasai, R.J. Bishop Jr., *J. Am. Chem. Soc.* 94 (1972) 5560–5566.
- [49] A. Sultana, R. Loenders, O. Monticelli, C. Kirschhock, P.A. Jacobs, J.A. Martens, *Angew. Chem. Int. Ed.* 39 (2000) 2934–2937.
- [50] Y. Li, T.L. Slager, J.N. Armor, *J. Catal.* 150 (1994) 388–399.
- [51] B.I. Mosqueda-Jimenez, A. Jentys, K. Seshan, J.A. Lercher, *Appl. Catal. B* 46 (2003) 189–202.
- [52] H.-Y. Chen, Q. Sun, B. Wen, Y.-H. Yeom, E. Weitz, W.M.H. Sachtler, *Catal. Today* 96 (2004) 1–10.
- [53] E.A. Lombardo, G.A. Sill, J.L. d'Itri, W.K. Hall, *J. Catal.* 173 (1998) 440–449.
- [54] N.W. Cant, I.O.Y. Liu, *Catal. Today* 63 (2000) 133–146.
- [55] A.D. Cowan, R. Dümpelmann, N.W. Cant, *J. Catal.* 151 (1995) 356–363.
- [56] D.B. Lukyanov, E.A. Lombardo, G.A. Sill, J.L. d'Itri, W.K. Hall, *J. Catal.* 163 (1996) 447–456.